Article

Bone Tissue Condition during Osteosynthesis of a Femoral Shaft Fracture Using Biodegradable Magnesium Implants with an Anticorrosive Coating in Rats with Experimental Osteoporosis

Yuliya V. Maistrovskaia [1], **Vera A. Nevzorova** [1], **Liyudmila G. Ugay** [1,*], **Sergey V. Gnedenkov** [2], **Evgeny A. Kotsurbei** [3], **Ekaterina A. Moltyh** [3], **Roman E. Kostiv** [4] and **Sergey L. Sinebryukhov** [2]

[1] Institute of Therapy and Instrumental Diagnostics, Pacific State Medical University, 690002 Vladivostok, Russia; mail@tgmu.ru (Y.V.M.); info@tgmu.ru (V.A.N.)
[2] Institute of Chemistry FEBRAS, 690022 Vladivostok, Russia; chemi@ich.dvo.ru (S.V.G.); sls@ich.dvo.ru (S.L.S.)
[3] Department of Pathological Anatomy and Forensic Medicine, Pacific State Medical University, 690002 Vladivostok, Russia; abit@tvgmu.ru (E.A.K.); plevra2008@rambler.ru (E.A.M.)
[4] Institute of Surgery, Pacific State Medical University, 690002 Vladivostok, Russia; kostiv2@rambler.ru
[*] Correspondence: lyudaugai.science@mail.ru

Abstract: Today, osteoporosis has become a major global health issues. The World Health Organization declares that 320 billion people have osteoporosis now, and more than 1.5 billion osteoporosis traumatic events occur every year. Bones become fragile and fracture risk is high; thus, it is crucial to choose the right biodegradable implants in order to minimize reoperations of patients with systemic osteoporosis. This investigation aimed to carry out a morphological assessment of the state of bone tissue with osteosynthesis of a femoral fracture in rats, using a model of osteoporosis with the installation of magnesium alloy implants coated with hydroxyapatite and sealed with polytetrafluoroethylene. According to this study, the indicators of angiogenesis and bone formation in experimental animals were significantly higher when an implant coated with hydroxyapatite sealed with polytetrafluoroethylene was used, compared to an implant coated only with hydroxyapatite and in rats without an implant. Based on the data obtained, it is possible to consider a magnesium implant coated with hydroxyapatite and sealed with polytetrafluoroethylene as a promising material for fracture therapy in patients with reduced bone density.

Keywords: osteoporosis; biodegradable implants; magnesium alloys; hydroxyapatite; polytetrafluoroethylene

1. Introduction

The important issue of modern traumatology and orthopedics is fast and effective fracture stabilization. Implants made of various materials and widely used as fixators can significantly improve the results of fracture treatment and arrange a sufficient rehabilitation potential to reconstruct lost bone functions. One of the problems when installing implants is the need to remove the structure after restoring the integrity of the bone. Re-surgical intervention makes all possible risks higher and may not always be completely successful, according to modern requirements in traumatology, a field has been established to model the study of the possibilities of using biodegradable implants. Implants made of materials that are biocompatible with human bone, have mechanical properties close to the bone, and completely resorb after effective synthesis of bone tissue and magnesium alloys are closest to these requirements.

A particular problem is the surgical treatment of fractures against the background of a decrease in bone density or in the presence of osteoporosis. Osteoporosis and associated fractures are an urgent medical and social problem. Osteoporosis is detected in 34% of

women and 27% of men, and the incidence of osteopenia is 43% and 44%, respectively, among people aged 50 years and older. These rates of osteoporosis have been reported among the white population of North America and several Western and Eastern European countries [1]. The incidence of osteoporosis increases with age [2]. In general, about 14 million people in the world suffer from osteoporosis, and another 20 million people have a decrease in BMD, corresponding to osteopenia [2].

The social significance of osteoporosis is determined by its consequences—fractures of the vertebral bodies and bones of the peripheral skeleton—leading to large material costs in the field of healthcare and causing a high level of disability and mortality.

Such fractures are characterized by delayed consolidation in 5–2% of cases and by the formation of false joints after surgical treatment in 30% of cases.

In patients with normal bone metabolism after osteosynthesis, increased bone resorption is combined with adequately increased bone formation, which leads to timely fracture consolidation; however, in patients with impaired bone tissue metabolism, the discrepancy between the intensity of these two processes significantly slows down fracture consolidation or leads to the formation of false joints. Repeated surgical intervention to remove the implant creates additional risks in this group of patients. Therefore, the evaluation of the effectiveness of the use of biodegradable implants in order to minimize re-interventions is of particular interest [3].

The classification of orthopedic implants inserted into the human body [3,4] could be made according to the time that the patient needs for recovery. There are permanent devices that are designed to be durable and replace human parts throughout the lifespan of the patient, as well as implants that require a second surgery in order to be removed (temporary implants). Sometimes, for the permanent prosthesis, revision surgery is necessary. For solving the problem of a temporary implant, biodegradable materials could be used. Current biodegradable implants are mainly made of resorbable polymers [5,6], bioceramics [7,8], or their combination [9–11]. However, poor mechanical strength of the polymers and brittleness of the ceramics often limit their application as load-bearing devices, and these materials are used as a scaffold for reconstruction of bone defects. The second trend is the use of metallic biodegradable materials for the fixation of fractured bone parts. To heal acceleration, broken bones must be firmly stabilized to avoid even micro-movements under the influence of applied forces. Implants made from some metals and alloys are preferred for load-bearing applications because of their superior mechanical strength near to human bone.

Magnesium and magnesium alloys exhibit good biocompatibility, mechanical strength, and biodegradation properties and may be used as materials for the production of temporary implants [5,12]. The products of the dissolving alloys are friendly to the human organism. Magnesium has an elastic modulus of about 45 GPa, a value close to that of bone (15–25 GPa). Mg alloy density is between 1.74 and 1.84 g/cm^3, depending on the alloying components, being almost equal to the one of human bone (1.8–2.1 g/cm^3). Unfortunately, magnesium alloys are susceptible to corrosion in physiological aqueous media and need protection [13]. Surface modifications are useful, mainly for slowing the corrosion process, but also for clinical needs regarding biodegradable Mg alloys. Special coatings need to be created on the magnesium surface to equilibrate the implant corrosion and bone tissue formation rates. From the electrochemical surface modification class, plasma electrolytic oxidation (PEO) forms a protective ceramic-like coating on the treated magnesium alloys [14–17]. The formation of calcium phosphate and polymer-containing coating are aimed at improving both the corrosion protection of the Mg alloy and at providing biocompatibility of the metallic implant [18].

According to results of prior in vivo experiments [19], magnesium alloy does not cause any negative effects during resorption in a rat body. Effects of long-term degradation of magnesium implants in vivo on continuous bone tissue growth in a rat skeleton were also reported [20]. Moreover, it is well accepted that coupling and synchronization of material resorption and bone healing is conducive in maintaining mechanical stability and

subtle biological responses, thereby achieving homeostatic balanced implant dissolution and complete osteosynthesis or reconstruction [21]. In this work, we used as a substrate the MA8 magnesium alloy with small amounts of alloying elements Mn (1.5–2.5 wt %) and Ce (0.15–0.35 wt %). This material is one of the slowly degrading magnesium alloys, and its alloying elements are not harmful to the human organism [15,22]. The authors found that bone recovers after complete degradation of the magnesium implants made from the alloys with manganese and rare earth elements. The degradation of the Mg alloys generates a significant increase in Mg concentration in the cortical bone near the remaining implant parts, but the Mg accumulation disappears after the implant degrades completely. Moreover, it was established that the hydrogen gas formation and ion release during magnesium implant degradation did not harm bone regeneration and the organism state in whole. The evacuation of degradation products from the organism was realized rather quickly.

Surgical treatment of fractures in patients with osteoporosis requires minimizing possible reoperations. Evaluation of the effectiveness of using biodegradable implants, in this case, is of particular interest [19].

This work aims to study the features of the reparative potential of bone tissue during osteosynthesis of a fracture in the femoral shaft in the case of using a magnesium implant with a bioactive layer and in the case of using a bioactive and anticorrosive layer. The studies were carried out on Wistar rats with a model of osteoporosis. In one group of rats, biodegradable magnesium alloy implants coated with hydroxyapatite without polytetrafluoroethylene were used. Another group used hydroxyapatite-coated implants sealed with polytetrafluoroethylene.

2. Materials and Methods

Samples of tissues of the femur from 26 white laboratory male Wistar rats from 180 to 240 g were used as material for the research. A model of experimental osteoporosis was reproduced in 24 animals by intragastric administration of prednisolone at a dose of 50 mg/kg under ether anesthesia for 14 days. Then, under aseptic conditions under anesthesia (zoletil 40 mg/kg of weight intraperitoneally), a closed fracture in the diaphyseal part of the femur was formed.

The screw-shaped implant with 26–30 mm of length and 2.0 and 2.3 mm of diameter was used for osteosynthesis.

The animals were divided into 4 groups of 6 individuals each. The implants for fracture stabilization were not used in the first group. The first group was used for comparison analysis (lilac color in the Figures).

In the second and third groups of rats under anesthesia (zoletil 40 mg/kg intraperitoneally), closed intramedullary retrograde osteosynthesis was performed. In the second group (colored turquoise in the Figures), a magnesium alloy implant (MA8) with a calcium–phosphate coating by plasma electrolytic oxidation was used for osteosynthesis [17].

In the third group (colored green in the Figures), the application of calcium–phosphate and composite polymer-containing coating used particles of superdispersed polytetrafluoroethylene (UPTFE) trademark "Forum®", obtained from the pyrolysis products of fluoroplastic F-4 using the technology of thermal gradient synthesis [23].

The control group was represented by the fourth group of rats with osteoporosis (dashed lines in the Figures), and two healthy individuals were used to confirm the presence of osteoporosis in rats of the experimental group.

The animals were withdrawn from the experiment on the 14th, 30th, and 60th days after the operation (200 mg zoletil). All experiments were performed following the rules of careful handling of laboratory animals required by standards of animal welfare and scientific research by Directive 2010/63/EU on protection of animals used for scientific purposes. The research procedure was approved by the independent interdisciplinary ethics committee of Pacific State Medical University.

Bone sections in the area of the fracture and the lumbar vertebrae were stained with hematoxylin and eosin, followed by morphological assessment of the state of bone tissue. Morphometric indicators were calculated using the ZEN program. Stained histological preparations were examined using an OLYMPUS BX41 microscope (OLYMPUS Corp., Tokyo, Japan). Microphotography was performed using the Levenhuk-ToupView-CD-2015-11 computer program. Quantitative analysis was performed using the computer program "ImageJ". One slice was cut from each sample of one bone, on which 3 fields of vision were examined.

The following parameters were assessed in this research:

1. Parameters reflecting the amount of bone tissue (volumetric density of trabeculae) with an assessment of mineralized bone tissue, osteoid, the so-called mineralized volume (trabecular bone volume, Tb.V, %), and the width of the cortical layer (cortical width, Ct.Wi, μm);
2. Static parameters reflecting the microarchitectonics of the cancellous bone (trabecular thickness, Tb.Th. μm);
3. The parameter of bone formation (the average thickness of the layers of the osteoid: osteoid thickness, O.Th., microns the number of osteoblasts; the number of osteoblasts, N.Ob.);
4. Parameters of resorption-eroded surface (ES, %) and the number of osteoclasts (N.Oc.) calculated per 1 square millimeter of bone section;
5. Average volumetric density of vessels (%).

The diameter of the vessels with the release of capillaries, arterioles, and venules was determined; then, the volumetric density of microvessels was calculated using the morphometric grid of A.G. Avtandilov with 289 intersections [24]. The counting of vessels was carried out with a magnification of the objective—×200, followed by normalization of their number per unit area. The number of measurements of each parameter for one slice was 10. Then, the mean value of the parameter and the standard error of measurements were determined.

The processing of quantitative data was carried out using the Excel program for Mac, version 14.5.7, using the capabilities of the Statistica 12.6 program (by Dell). The Mann–Whitney test was used to analyze the differences. Differences were considered significant at $p < 0.01$ [25].

3. Results

Based on the purpose of the research, we analyzed the state of bone tissue in three groups of animals with a fracture in the femoral shaft. The bone repair was assessed on days 14, 30, and 60 of the experiment. The control group consisted of animals with a model of osteoporosis without fracture.

The morphological picture of the bone tissue of the femur in animals with a model of osteoporosis, withdrawn from the experiment on day 14, was characterized by thinning of the bone trabeculae with a decrease in the volumetric density of bone tissue due to an increase in the volumetric density of the resorbable surface. Osteolytic changes predominated in the most active cancellous part of the bone tissue. Expansion of the canals of the Haversian system with filling with fibroreticular tissue was clearly observed. The identified morphological changes in bone tissue are typical for osteoporosis [26].

The changes in bone tissue described above were found in all groups of animals that completed the experiment by day 14. In the study of calluses in the group of rats with a fracture without placing an implant, an insignificant restoration of the volume of the damaged bone was noted. In the projection of the putative callus, fibroreticular tissue with single small foci of the osteoid and slit-like vessels predominates. The centers of regeneration are located endosteally. Bone formation in this group is incomplete; the newly formed osteoid is scarce, formed by a few osteoblasts that are in the active phase of osteogenesis. Mineralization of the newly formed osteoid in animals of this group was not found. In the remaining areas, the mature lamellar bone had pronounced periostocytic resorption, thinning of bone trabeculae, uneven arrangement of osteocytes, a large number

of Gauship lacunae, which was empty, and containing osteoclasts (Figure 1a); in the preparations, axillary resorption was noted with an increase in the space between the plates (Figure 1a).

(a)   (b)   (c)
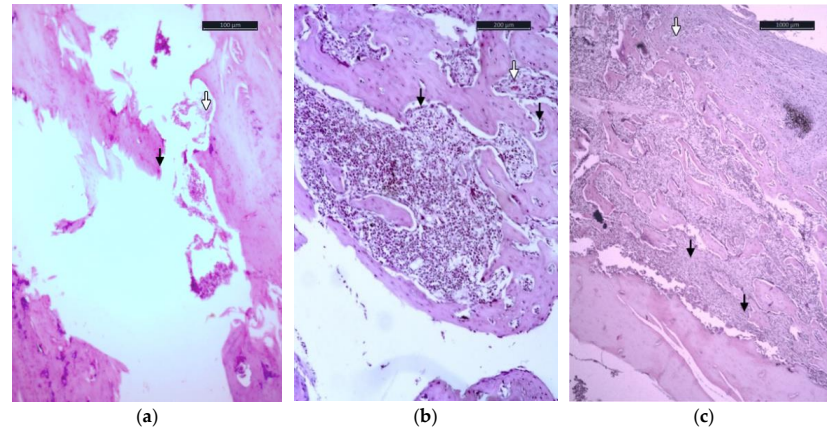
Figure 1. Bone tissue of a rat in the area of a hip shaft fracture on the 14th day of the experiment: (**a**) rat without an implant; HE ×400; (**b**) rat with magnesium implants coated with hydroxyapatite; HE ×400; (**c**) rat with a magnesium implant coated with hydroxyapatite and sealed with polytetrafluoroethylene (the arrow marks the focus of perichondral osteogenesis; the medullary part of the bone is filled with fibroreticular tissue →), empty Gauship lacunae containing osteoclasts (marked with an arrow ⇒). Staining with hematoxylin and eosin at constant magnification HE ×100.

In the third group of rats, the cortical part of the bone in the damaged area was filled with cartilage (Figure 1c). Focuses of perichondral osteogenesis were noted in the endosteal part of the defect (Figure 1c).
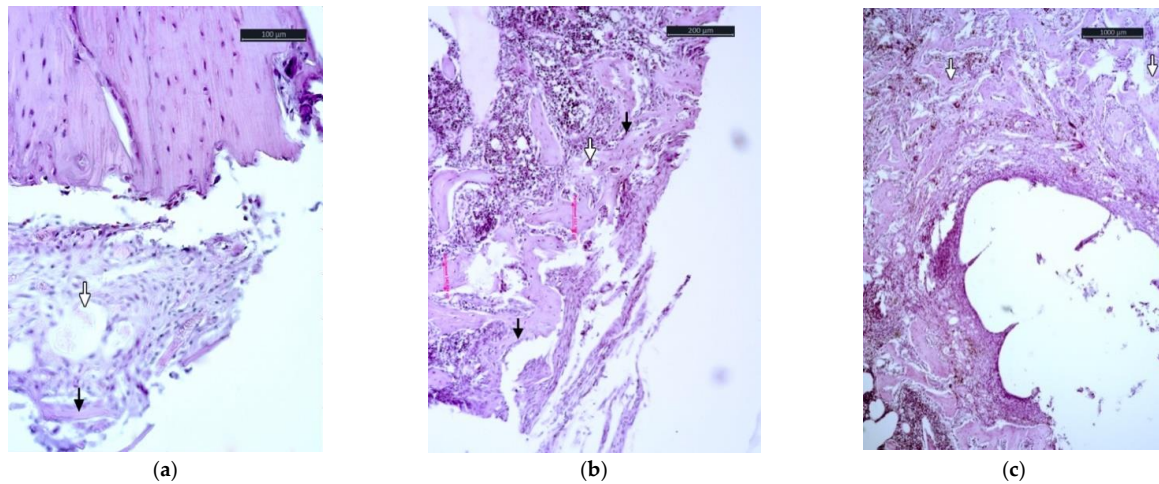
On the 30th day of the experiment, the difference in the morphological picture of the bone tissue of the three groups of animals remained. In the first group (without an implant), the damaged area was filled with fibroreticular tissue, among which were osteoid microfoci (Figure 2a). Osteoblasts were located on the surface of forming bone plates, among fibroreticular tissue, and in the projection of vascular pericytes, but their number did not increase compared to the control. The mineralization of the osteoid was not established.

The bone tissue of the second group of animals (the implant covered with hydroxyapatite) was distinguished by more pronounced proliferative processes. Bone defects were completely filled with a fibroreticular component, among which there was differentiated elements of cancellous bone (Figure 2b). Among the fibroreticular tissue, single vessels of the capillary type were noted.

The use of magnesium implants with hydroxyapatite sealed with polytetrafluoroethylene in experimental animals led to complete stabilization of the damaged area with the filling of fibroreticular tissue, among which there were structured elements of already lamellar cancellous bone (Figure 2c). At the same time, osteogenesis continued, which was reflected in the growing numbers of cells in the osteoblastic pool. The distribution of the mineral component was regulated by different activities of osteoclasts. The latter was located in Gauship gaps in both the active (multinuclear population) and inactive (single-core) phases.

On the 60th day of the experiment, the bone defect was filled with fibroreticular bone, the bulk of which was the fibrous component in the group of rats without an installed implant. Among the fibrous tissue lay complexes of the bone lamina, locally joining together to form cancellous bone structures (Figure 3a). Nevertheless, against this background, zones of the type of osteogenesis imperfecta were identified, which was identified as the chaotic arrangement of bone trabeculae surrounded by active osteoblasts. Violation of the smooth edge of the bone trabeculae was associated with the increasing volumetric density of the

eroded surface of the bone trabeculae (Table 1). This fact was due to the lack of a mineral component in the bone tissue under construction. This shortage was compensated by the local depot.

(a)   (b)   (c)

Figure 2. Bone tissue of a rat in the area of a fracture in the femoral diaphysis on the 30th day of the experiment: (**a**) a rat without an implant; in the area of damage among the fibroreticular tissue of the osteoid stripes (marked with an arrow →), capillary vessels, pericytes of the latter with the onset of transformation into osteoblasts (marked with an arrow ⇒); HE ×400. (**b**) a rat with magnesium implants coated with hydroxyapatite; among the fibroreticular tissue, there are bone trabeculae with thin osteoid stripes on the surface and chains of osteoblasts (marked with an arrow →), slit-shaped vessels (marked with an arrow ⇒); HE ×200. (**c**) a rat with a magnesium implant covered with hydroxyapatite sealed with polytetrafluoroethylene; an oblique defect with a picture of the pronounced transformation of the fibroreticular bone into a lamellar spongy bone (arrows mark the formed bone beams). Staining with hematoxylin and eosin, at constant magnification; HE ×100.

(a)   (b)   (c)
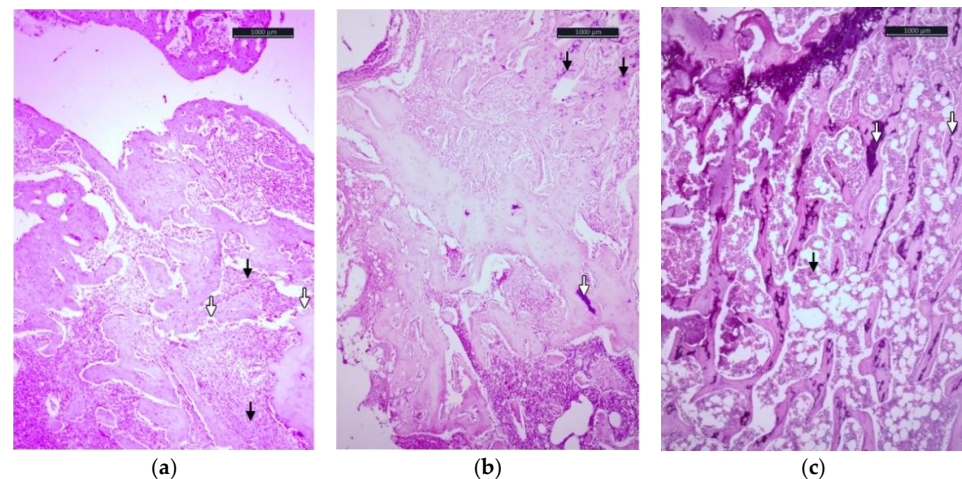
Figure 3. Bone tissue of a rat in the area of a fracture in the femoral diaphysis on the 60th day of the experiment: (**a**) rat without an implant: chains of osteoblasts on the surface of bone trabeculae (marked with arrows ⇒); among fibrous tissue, foci with osteogenesis imperfecta (marked with an arrow →); HE ×100. (**b**) rat with magnesium implants coated with hydroxyapatite: bone mineralization (marked with arrows ⇒), focus of perichondral ossification (marked with an arrow →); HE ×100. (**c**) a rat with a magnesium implant coated with hydroxyapatite, sealed with polytetrafluoroethylene: lamellar cancellous bone with filling of the interbeam space with bone marrow (marked with an arrow →), bone trabeculae with completed mineralization (marked with arrows ⇒). Staining with hematoxylin and eosin at constant magnification; HE ×100.

Table 1. Indicators of morphometry of the femur of rats with a fracture in the shaft of the bone.

Indicator	Rats with Osteoporosis Model (Control Group) $n = 6$	14-Day Experiment			30-Day Experiment			60-Day Experiment		
		Group 1 $n = 2$	Group 2 $n = 2$	Group 3 $n = 2$	Group 1 $n = 2$	Group 2 $n = 2$	Group 3 $n = 2$	Group 1 $n = 2$	Group 2 $n = 2$	Group 3 $n = 2$
CW (cortical width. μm)	146.2 ± 0.3	129.7 ± 3.4	136.6 ± 4.5	152.5 ± 4.9	133.2 ± 5.3	138.3 ± 2.9	142.9 ± 3.0	134.1 ± 5.5	146.8 ± 1.9	150.3 ± 8.6
TT (thickness of trabeculae. μm)	53.3 ± 2.2	55.3 ± 4.4	56.8 ± 7.6	54.8 ± 6.3	44.5 ± 1.7	47.8 ± 7.6	57.3 ± 8.1	49.7 ± 1.3	69.4 ± 1.7	67.6 ± 4.1
N.Ob (number of osteoblasts. in mm^2)	9.1 ± 0.7	4.6 ± 1.07	3.8 ± 0.97	9.2 ± 1.77	3.2 ± 0.89	4.4 ± 2.4	14.6 ± 2.1	3.4 ± 1.4	6.4 ± 2.4	11.6 ± 2.1
ES (eroded surface) %	4.7 ± 2.1	6.9 ± 3.4	6.6 ± 1.3	6.0 ± 3.1	17.3 ± 4.3	14.3 ± 4.4	6.8 ± 3.6#	16.4 ± 3.1	6.1 ± 2.8	4.6 ± 2.4
N.Oc (number of osteoclasts. (in mm^2)	1.8 ± 1.3	5.2 ± 1.7	2.8 ± 1.2	3.6 ± 1.1	6.3 ± 1.4	7.3 ± 5.2	3.4 ± 0.7	5.8 ± 0.9	4.5 ± 1.8	1.8 ± 0.1
Average volumetric density of vessels%	13.2 ± 1.9	13.67 ± 1.003	18.1 ± 1.78	22.8 ± 1.46	14.7 ± 1.6	21.9 ± 2.03	26.4 ± 3.2	15.1 ± 1.7	23.3 ± 2.4	29.6 ± 3.7

The use of magnesium implants on day 60 promoted perichondral osteogenesis (Figure 3b). The space between the bone beams began to fill with bone marrow content. The bulk density of the eroded surface decreased and approached the control values. Mineralization focuses were fixed.

The third group of animals in the area of installation of a magnesium implant coated with hydroxyapatite and sealed with polytetrafluoroethylene had differentiated bone tissue of a lamellar spongy character in its structure. The differentiation of the fibroreticular tissue was completed, and the bone marrow space was filled with bone marrow. The eroded surface was practically not detected. The zones of transition of the cancellous bone to the compact were formed.

In the bone tissue of animals in groups with different types of implants (groups 2 and 3), the morphological picture does not differ significantly (Figure 3b,c). The areas of the defect are practically restored and are represented by lamellar bone with a system of osteons and Haversian canals. The cancellous bone is transformed into a compact one, and the thickness of the cortical layer increases. The activity of single osteoclasts, forming lacunae of resorption in the projection of osteogenesis and the distal regions from the fracture site, was noted.

One of the main stages of bone tissue restoration is angiogenesis—the formation and growth of blood vessels that provide oxygenation, migration, and "homing" in the damaged area of progenitor cells capable of differentiation in the osteoblastic direction [27]. To assess angiogenesis, we used an indicator of the average volumetric density of the vessels. The results of measuring the parameters are presented in Table 1.

4. Discussion and Results

According to the data obtained, as early as on the 14th day of the study, the average volumetric density of blood vessels in the third group of animals using magnesium implants coated with hydroxyapatite and polytetrafluoroethylene was higher compared to the indicators of animals in which simple magnesium implants were used with hydroxyapatite and animals without implantation. A graph of changes in the value of the volumetric density of vessels in the investigated groups of animals, depending on the time, is shown in Figure 4.
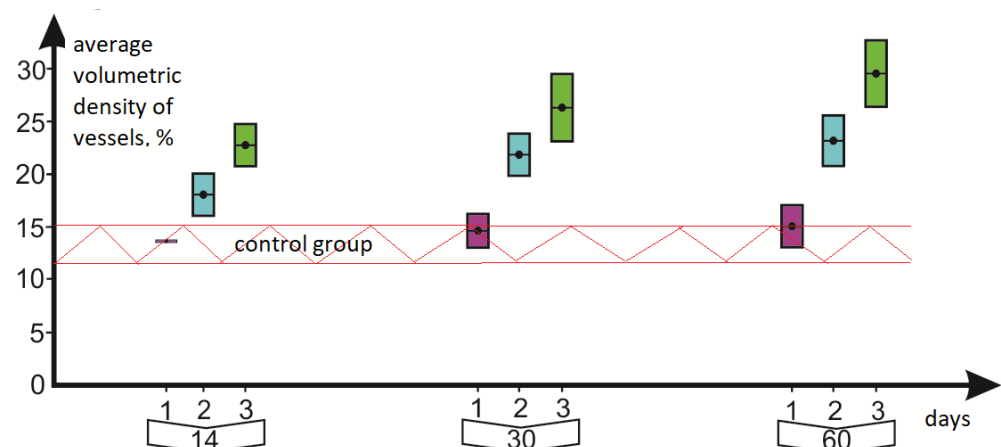
Figure 4. Change in the value of volumetric density of blood vessels in the investigated groups, depending on the time.

The vertical axis represents volumetric density of the vessels in %, and the horizontal axis is the time elapsed after the installation of the implants. Red dashed lines show the limits of changes in the values of the volumetric density of vessels in the control group (limits determined by the measurement error). Bulk density measurements were made on days 14, 30, and 60. The first group corresponds to the lilac color, the second group to turquoise, and the third to green. The length of the rectangles corresponds to the root-mean-

square error in measuring the volumetric density of the vessels. Exceeding the average values is beyond the limits of measurement errors both when comparing the results of the third group with the first group, and with the second group. Volumetric density of blood vessels in the third group exceeded the values in the control group by the 14th day. This trend persisted both on the 30th and 60th day of the study.

In the comparison group, the process of angiogenesis was weakly expressed, and the volumetric density of blood vessels throughout the entire time remained within the values of the control group. While in the second and third groups, angiogenesis was stimulated by the deposited calcium phosphate coating. Because the anticorrosive layer of polytetrafluoroethylene is applied, the process of formation and growth of blood vessels occurring more efficiently is clearly determined. Already on the 14th day, the volumetric density of vessels in the third group exceeded the values in the second group; this tendency persisted by the 60th day of the experiment.

Similar behavior was observed for other parameters that are important for the process of bone osteosynthesis in fractures. The dynamics of the width of the cortical layer–CW is shown in Figure 5, the vertical axis represents thickness of the cortical layer in microns, the rest of the designations and colors are the same as for Figure 4. In group 3, the width of the cortical layer by 14 days exceeded the values determined in the control group, which had an excess of measurement errors. By the 30th day, there was a slight decrease in the average CW value and it fell into the error of measuring the values of the control group. However, by day 60, the CW value in the third group reached its maximum value. This parameter for the second group of animals reached the values of the control group only by 60 days. Thus, this demonstrates the fact that the anticorrosive coating creates more favorable conditions for bone osteosynthesis in osteoporosis than when only the bioactive layer with hydroxyapatite is used.
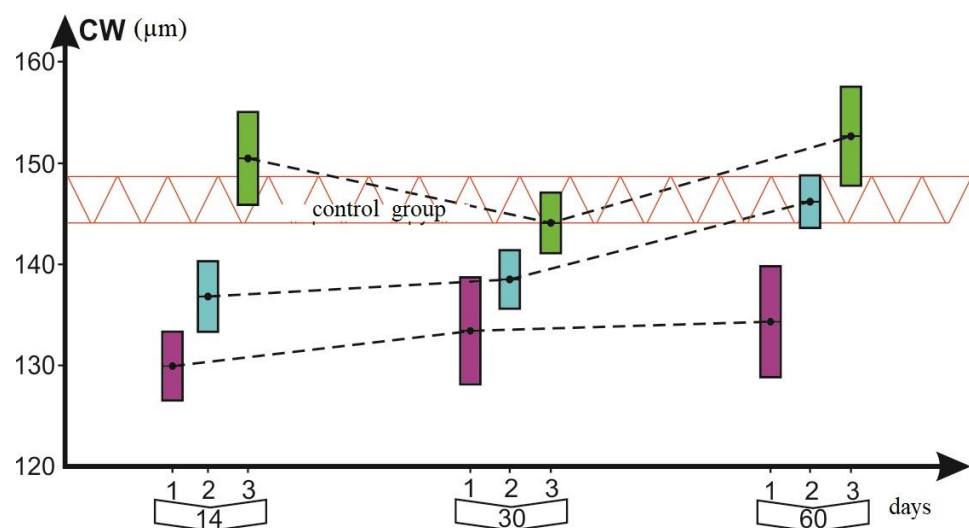

Figure 5. Dynamics of the thickness of the cortical layer for the studied groups of animals.

Perhaps this phenomenon is associated with the properties of the coatings to prevent the development of the inflammatory effect associated with the rapid resorption of magnesium from the implant, as noted by Chen et al. However, in this research, the osteoimmunomodulatory properties of implants were not studied. This study aims to evaluate the effectiveness of the osteoregeneration process using hydroxyapatite and tetrafluoroethylene deposited on a magnesium implant. Possibly, more efficient regeneration with the use of polytetrafluoroethylene is associated with favorable osteoimmunomodulatory properties of the biomaterial, the development of which is a promising strategy.

The CW values in the comparison group (group 1) did not reach the values of the control group by 60 days.

The graph in Figure 6 shows the dynamics of another parameter, N.Ob, which is important for osteosynthesis, with the number of osteoblasts in mm^2 on the cut surface. By the beginning of measurements on the 14th day, the number of osteoblasts was already within the measurement range of this parameter in the control group. At the same time, the values of the first two groups were less than the control values. Only by the 60th day in group 2, where implants with hydroxyapatite are used, did the N.Ob value approach the control one. After 14 days, the N.Ob values in the third group exceeded the values of the second and control groups (concerning the measurement error).
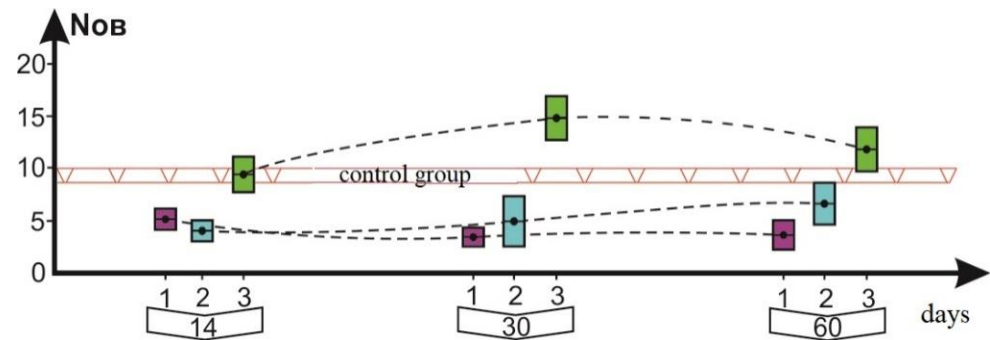
Figure 6. Changes to parameter N.Ob. The designations and colors on the graph correspond to those shown in Figure 4.

The analysis of changes in parameters TT, ES, and N.Oc shows their more complex temporal dynamics. The dynamics of the parameter TT (the vertical axis represents thickness of the trabeculae in microns) is shown in Figure 7 as an example. It is impossible to unequivocally interpret the increase in their mean values in group 3 over groups 1 and 2 overtime. Moreover, by the 60th day, the values of the TT parameter are aligned in the second and third groups. Apparently, the application of the antioxidant layer is not critical. The application of the calcium–phosphate layer has a more significant effect on its dynamics.
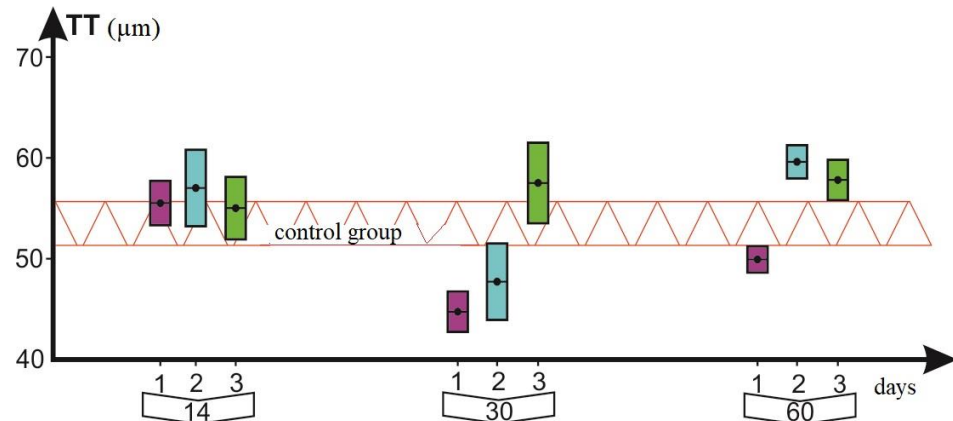
Figure 7. Trabeculae thickness dynamics. The colors and designations are the same as for Figure 4.

In this case, by the 14th day, the average values of all four groups of animals coincided with the limits of the measurement errors. By the 30th day, the same happened regarding the excess of parameters in group 3; however, by the 60th day, the TT values in the second and third groups equalized.

Figures 8 and 9 show the graphs of the dynamics of the parameters ES and N.Oc, respectively.
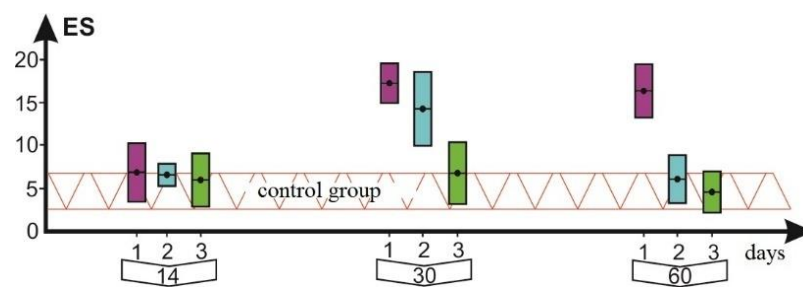
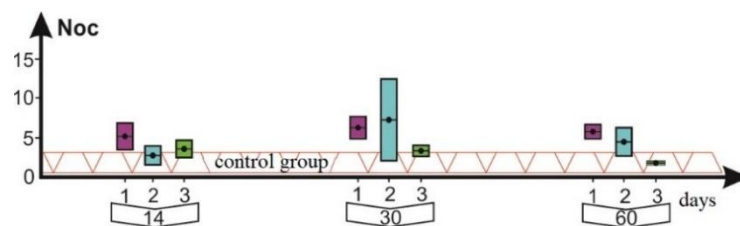**Figure 8.** Eroded surface dynamics (ES).

Figure 9. Dynamics of the number of osteoclasts (N.Oc).

Both of these parameters characterized the process of bone resorption and did not show any characteristic feature for the second and third groups. The N.Oc parameter remained practically constant in all three groups with values close to the control group. Both parameters in the comparison group begin to exceed the values of the control group already on the 30th day. What is the expected result for resorption in the case of the control group?

5. Conclusions

The search for biodegradable materials for use in osteosynthesis is one of the most promising areas in traumatology. A conventionally "ideal" composite should be completely metabolized by the body, without exerting local and systemic pathological effects, have the properties of "biocompatibility" with bone tissue, have sufficient strength, and at the same time, participate in accelerating the processes of bone tissue regeneration [27].

Partially magnesium biodegradable structures meet the listed requirements, but the issue of corrosion forces researchers to continue the search for coatings that can not only stop the corrosion of implants but can also contribute to the acceleration of osteogenesis [28,29]. One of the promising directions in the creation of such coatings is the use of hydroxyapatite coatings. According to Sae-Mi Kim et al. [15], a significantly lower rate of biocorrosion was observed in comparison with uncoated magnesium implants when rats were implanted in the skull bone of magnesium implants coated with hydroxyapatite. The same authors, in an experiment on rabbits, established a more active formation of bone tissue around magnesium implants with a hydroxyapatite coating during osteosynthesis of a tibial defect in comparison with uncoated magnesium implants at 6 and 12 weeks of the study.

In our study in rats with experimental osteoporosis, the use of magnesium implants with hydroxyapatite coatings for osteosynthesis of a femoral fracture also led to accelerated bone regeneration compared to rats without the use of implants. An interesting fact is that in the case of using magnesium implants with an anti-corrosive coating on the 14th and 30th days of the experiment, the osteosynthesis processes were more pronounced, in comparison not only with animals without implants, but also in comparison with constructions with hydroxyapatite coating.

Similar data were obtained in the work of Vasconelos M., Afonso A. et al. [30] in an experiment on rabbits, in which an artificially created defect of the tibia was coated with polytetrafluoroethylene-coated hydroxyapatite granules in one group and uncoated hydroxyapatite granules in the other. A month after the operation, the rabbits of the first group showed a more pronounced increase in the volumetric density of the cancellous bone in comparison with the group without polytetrafluoroethylene coating.

The mechanisms of the higher regenerative potential of the bone in the presence of polytetrafluoroethylene coating require deeper research. One of the possible options for the implementation of the coating effect can be the more pronounced angiogenesis obtained in our research at the fracture site in this group of animals, which is evidenced by the indicators of the average volumetric density of the vessels (Table 1).

According to our data, the average volumetric vascular density was significantly higher in the group of rats with a magnesium implant with an anti-corrosive coating on the 14th, 30th, and 60th days of the experiment, than in the rats with the implant with hydroxyapatite application. It is known that the formation of endochondral bone depends on the intensity of angiogenesis and stops if it is blocked, which is shown in models of experimental pathological conditions. In the experiment, inhibition of chondrocyte VEGF signals by blocking antibodies to a related receptor on developing vessels in the metaphysis leads to a stop not only of bone growth but also of chondrogenesis zones. A similar picture is observed in rickets, which can be mimicked by microsurgical ablation of the vascular system of the metaphysis [31].

Thus, according to our data, the most harmonious processes of the regenerative potential of bone tissue and its surroundings during osteosynthesis of fractures in difficult conditions of osteoporosis were observed when using biodegradable magnesium alloy implants with a hydroxyapatite coating, sealed with polytetrafluoroethylene. It should be understood that the translation of data on the processes of osteoregeneration in the experiment in rats to humans is limited, but the results obtained regarding morphological changes in bone tissue and angiogenesis give hope for the possibility of further promising studies in this direction.

References

1. Kanis, J.A.; Cooper, C.; Rizzoli, R.; Reginster, J.Y. Scientific Advisory Board of the European Society for Clinical and Economic Aspects of Osteoporosis (ESCEO) and the Committees of Scientific Advisors and National Societies of the International Osteoporosis Foundation (IOF). European guidance for the diagnosis and management of osteoporosis in postmenopausal women. *Osteoporos Int.* **2019**, *30*, 3–44. [CrossRef] [PubMed]
2. Reginster, J.Y.; Burlet, N. Osteoporosis: A still increasing prevalence. *Bone* **2006**, *38* (Suppl. 1), 4–9. [CrossRef] [PubMed]
3. Eglin, D.; Alini, M. Degradable polymeric materials for osteosynthesis: Tutorial. *Eur. Cell Mater.* **2008**, *16*, 80–91. [CrossRef] [PubMed]
4. Kannan, M.B.; Raman, R.K. In vitro degradation and mechanical integrity of calcium-containing magnesium alloy in modified simulated body fluid. *Biomaterials* **2008**, *29*, 23062314. [CrossRef]
5. Antoniac, I.; Miculescu, M.; Manescu, V.; Stere, A.; Quan, P.H.; Paltanea, G.; Robu, A.; Earar, K. Magnesium-Based Alloys Used in Orthopedic Surgery. *Materials* **2022**, *15*, 1148. [CrossRef]
6. Donnaloja, F.; Jacchetti, E.; Soncini, M.; Raimondi, M.T. Natural and Synthetic Polymers for Bone Scaffolds Optimization. *Polymers* **2020**, *12*, 905. [CrossRef]
7. Wang, Z.; Ma, Y.; Wang, Y.; Liu, Y.; Chen, K.; Wu, Z.; Yu, S.; Yuan, Y.; Liu, C. Urethane-based low-temperature curing, highly-customized and multifunctional poly(glycerol sebacate)-co-poly(ethylene glycol) copolymers. *Acta Biomater.* **2018**, *71*, 279–292. [CrossRef]

8. Jeong, J.; Kim, J.H.; Shim, J.H.; Hwang, N.S.; Heo, C.Y. Bioactive calcium phosphate materials and applications in bone regeneration. *Biomater. Res.* **2019**, *23*, 4. [CrossRef]

9. Liu, Y.; Ma, Y.; Zhang, J.; Xie, Q.; Wang, Z.; Yu, S.; Yuan, Y.; Liu, C. MBG-Modified β-TCP Scaffold Promotes Mesenchymal Stem Cells Adhesion and Osteogenic Differentiation via a FAK/MAPK Signaling Pathway. *ACS Appl. Mater. Interfaces* **2017**, *9*, 30283–30296. [CrossRef]

10. Ma, Y.; Zhang, C.; Wang, Y.; Zhang, L.; Zhang, J.; Shi, J.; Si, J.; Yuan, Y.; Liu, C. Direct three-dimensional printing of a highly customized freestanding hyperelastic bioscaffold for complex craniomaxillofacial reconstruction. *Chem. Eng. J.* **2021**, *411*, 128541. [CrossRef]

11. Borsch, C.; Melsen, B.; Vargrvic, K. Guided bone regeneration in calvarian bone defects using polytetrafluoroethylene membranes. *Cleft Palate Craniofacial J.* **1995**, *32*, 311.

12. Kamrani, S.; Fleck, C. Biodegradable magnesium alloys as temporary orthopaedic implants: A review. *BioMetals* **2019**, *32*, 185–193. [CrossRef] [PubMed]

13. Brar, H.S.; Platt, M.O.; Sarntinoranont, M.; Martin, P.I.; Michele, V. Magnesium as a Biodegradable and Bioabsorbable Material for Medical Implants. *Biomed. Mater. Devices* **2009**, *61*, 31–35. [CrossRef]

14. Gnedenkov, S.V.; Sharkeev, Y.P.; Sinebryukhov, S.L.; Khrisanfova, O.A.; Legostaev, E.N.; Zavidnaya, A.G.; Puz, A.V.; Khlusov, I.A. Functional Coatings for Implant Materials. *Pac. Med. J.* **2012**, *1*, 12–20.

15. Kim, S.-M.; Jo, J.-H.; Lee, S.-M. Hydroxyapatite-coated magnesium implants with improved in vitro and in vivo biocorrosion, biocompatibility, and bone response. *J. Biomed. Mater. Res.* **2014**, *102*, 429–440. [CrossRef] [PubMed]

16. Barrère, F.; de Groot, B.K. Bone regeneration: Molecular and cellular interactions with calcium phosphate ceramics. *Int. J. Nanomed.* **2006**, *1*, 317–332.

17. Gnedenkov, S.V.; Sinebryukhov, S.A.; Khrisanfova, O.A.; Zavidnaya, A.G.; Egorkin, V.S.; Puz, A.V.; Sergienko, V.I. Calcium phosphate coatings on resorbable magnesium implants. *Bull. Far East Branch Russ. Acad. Sci.* **2011**, *5*, 88–96.

18. Iscandar, M.E.; Aslani, A. The effect of nanostructured hydroxyapatite coating on the biodegradation and cytocompatibility of magnesium implants. *J. Biomed. Mater. Res. Part A* **2013**, *101*, 2346–2352. [CrossRef]

19. Plekhova, N.G.; Lyapun, I.N.; Gnedenkov, S.V.; Sinebryukhov, S.L.; Mashtalyar, D.V. The role of dendritic cells in bone loss and repair. In *Dendritic Cells*; Chapoval, S.P., Ed.; IntechOpen: London, UK, 2018; pp. 79–99. [CrossRef]

20. Amerstorfer, F.; Fischerauer, S.F.; Fischer, L.; Eichler, J.; Draxler, J.; Zitek, A.; Meischel, M.; Martinelli, E.; Kraus, T.; Hann, S.; et al. Long-term in vivo degradation behavior and near-implant distribution of resorbed elements for magnesium alloys WZ21 and ZX50. *Acta Biomater.* **2016**, *42*, 440–450. [CrossRef]

21. Niu, H.; Ma, Y.; Wu, G.; Duan, B.; Wang, Y.; Yuan, Y.; Liu, C. Multicellularity-interweaved bone regeneration of BMP-2-loaded scaffold with orchestrated kinetics of resorption and osteogenesis. *Biomaterials* **2019**, *216*, 119216. [CrossRef]

22. Lim, H.-K.; Byun, S.-H.; Lee, J.-Y. Radiological, histological, and hematological evaluation of hydroxyapatite-coated resorbable magnesium alloy screws placed in rabbit tibia. *J. Biomed. Mater. Res.* **2017**, *105*, 1636–1644. [CrossRef] [PubMed]

23. Tsvetnikov, A.K.; Uminsky, A.A.; Kulikov, A.P.; Falaleev, O.F. Study on intercalation of platinum hexafluoride in thermoexpanded graphite. In *Materials Science Forum*; Trans Tech Publications: Schwyz, Switzerland, 1992; Volume 91/92, pp. 107–111.

24. Avtandilov, G.G.; Yabluchanskii, I.; Gubenko, G. Planimetric grids for macroscopic and microscopic stereological investigations. *Bull. Exp. Biol. Med.* **1977**, *83*, 111–113. [CrossRef]

25. Hart, A. Mann-Whitney test is not just a test of medians: Differences in spread can be important. *BMJ* **2001**, *18*, 391–393. [CrossRef]

26. Riggs, B.L.; Melton, J., III. *Etiology, Diagnosis, and Management*, 3rd ed.; Lippincott Williams & Wilkins: Philadelphia, PA, USA, 1995; pp. 457–479.

27. Hankenson, K.D.; Dishowitz, M.; Gray, C.; Schenker, M. Angiogenesis in bone regeneration. *Injury* **2011**, *42*, 556–561. [CrossRef] [PubMed]

28. Marenzana, M.; Arnett, T.R. The Key Role of the Blood Supply to Bone. *Bone Res.* **2013**, *3*, 203–215. [CrossRef] [PubMed]

29. Kim, J.H.; Park, Y.S.; Oh, K.J.; Choi, H.S. Surgical treatment of severe osteoporosis including new concept of advanced severe osteoporosis. *Osteoporos. Sarcopenia* **2021**, *7*, 89–120. [CrossRef]

30. Vasconelos, M.; Afonso, A.; Branco, R. Guided bone regeneration using osteopatite granules and polytetrafluoroethylene membranes. *J. Mater. Sci. Mater. Med.* **2004**, *8*, 815–818. [CrossRef]

31. Hunter, W.L.; Arsenault, A.L.; Hodsman, A.B. Rearrangement of the metaphyseal vasculature of the rat growth plate in rickets and rachitic reversal: A model of vascular arrest and angiogenesis renewed. *Anat. Rec. Adv. Integr. Anat. Evol. Biol.* **1991**, *229*, 453–461. [CrossRef]